2024 European Control Conference (ECC)
June 25-28, 2024. Stockholm, Sweden

Structure and Parameters Estimation of Complex Grid Impedance

Amin Rezaeizadeh[1], Silvia Mastellone[1], Federico Bertoldi[2] and Peter Al Hokayem[2]

Abstract— **This paper presents a novel frequency-based method to estimate the structure and parameters of a grid equivalent model by measuring currents and voltages at the terminals of the point of common coupling. This model is instrumental in calibrating the controller of grid connected power converters. The proposed approach is demonstrated on the two most common equivalent grid structures of second and forth order respectively, and can be generalized to arbitrary grid order. Additionally, the method provides a measure to assess the quality of available data for estimation purposes, and therefore to determine the estimation feasibility with the given data-set.**

I. INTRODUCTION

Power electronics converters are estimated to process around 70% of the world's electricity and this figure is expected to further increase with the integration of renewable energy sources in the grid. They enable reliable and efficient power transfer for a wide range of applications across various industries such as mobility, oil and gas, renewable energy and power generation.

Traditionally, power grids were characterized by high inertia and of relative strong or fixed nature, which allowed the operation of power converters by proper calibration of their controllers during the commissioning phase. Nowadays, frequent changes in the grid structure and strength require the controllers to be reconfigured online based on estimated grid impedance which helps preserve stability and optimal performance, see, for example, stability analysis [1, 2], voltage control [3]–[5], adaptive current controller [6] and islanding detection for protection purposes [7, 8].

Identification methods can be generally categorized into passive and active ones. Passive techniques estimate the grid impedance using the available voltage and current at the point of common coupling (PCC) without any additional signal injection into the grid [9]. They include state observers [10], Kalman filters [11, 12] and least-squares solutions [8, 13]. In contrast, active methods require the injection of an additional signal perturbation into the grid with the risk of disturbing the connected converter(s) away from normal operation. These approaches include variation of the converter operating points [12, 14]–[16], and frequency-based injection [3, 5, 17]–[26]. In both cases the quality of the estimation is highly dependent on the data frequency content and quality. This aspect is however not directly addressed in the existing methods, as they provide no explicit criteria nor analysis tools to assess the data quality with respect to identification feasibility and accuracy. Moreover, most of the approaches in the referenced works focus on first-order grid models, e.g., RL-type (resistor-inductor), and do not include higher-order models, for example, LCL-type (inductor-capacitor-inductor) grid models that are quite common wind power generation applications. Finally, the above methods already assume a fixed grid structure and focus on the estimation of the parameters.

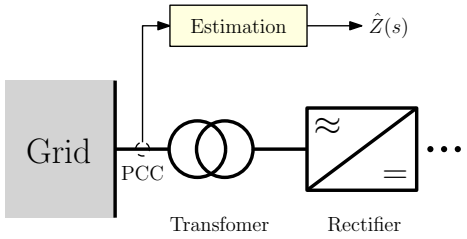

Fig. 1. Measuring electric signals at the point of common coupling and estimating an equivalent grid impedance.

The contribution of this paper is to bridge the aforementioned gaps and provide an effective, accurate and efficient method to identify the structure and parameters of higher-order equivalent grids. Moreover, it provides a measure of the estimation accuracy based on data quality. We assume that measurements of voltages and currents with an appropriate sampling rate are available at the PCC (see Fig. 1). Based on the measured data, we present a novel frequency-based impedance estimation approach that identifies the structure and parameters of the underlying grid, and in the process an assessment of the feasibility of estimation based the "richness of the measured data". The frequency-domain nature of the approach allows to eliminate measurement noise or ineffective frequency content from the signals prior to the estimation process. This improves robustness, efficiency and accuracy of the estimation.

The remainder of this article is organized as follows: Section II describes the system under consideration and formulate the identification problem. Section III is devoted to describe the main paper contribution and the details of the proposed method. Section IV then describes the algorithm steps and Section V demonstrates the method effectiveness on a concrete example. Section VI provides conclusive remarks and remarks on potential future work.

This work was supported by the Swiss National Science Foundation under NCCR Automation, grant agreement 51NF40_180545

[1]Amin Rezaeizadeh and Silvia Mastellone are with the Institute of Electric Power Systems, University of Applied Science Northwest Switzerland, Windisch, Switzerland. amin.rezaeizadeh@fhnw.ch, silvia.mastellone@fhnw.ch

[2]Federico Bertoldi and Peter Al Hokayem are with ABB Motion, ABB Switzerland Ltd., Turgi, Switzerland. federico.bertoldi@ch.abb.com, peter.al-hokayem@ch.abb.com

II. Problem statement and system modeling

A typical by-directional, grid-connected power conversion system setup includes the power grid with a transformer and input/output filter, the power converter with a motor or generator and finally the load. The filters, transformers and machine parameters are typically known by the converter that optimally calibrate its operation based on those parameters. The grid characteristics after the transformer are however unknown to the converter, (see Fig. 1), so an initial calibration is performed during the commission phase to guarantee stable operation for the specific grid.

This approach is sufficiently reliable for conventional stable and predictable grids. However, for the new generation of grids, populated by intermittent generation and loads elements and characterized by unpredictability and high dinamicity, one converter controller configuration cannot optimally provide the performance requirements under all different transient and steady state operating conditions. This leads at best to under performance and often to compromised stability and reliability of the system.

A consistently updated knowledge of the changes affecting the grid can support the online reconfiguration of the converter controller leading to a more reliable and stable operation.

This paper considers two of the most common grid equivalent models used to calibrate converter controllers during commissioning the RL and LCL circuit depicted in figure 2. Given voltage and current measured at the converter point of common coupling, V_{pcc} and I_{pcc} respectively, an unknown grid voltage V_g at 50Hz frequency, we need to identify the grid structure (RL or LCL) and parameters, characterize the estimation accuracy based on signals frequency content, and finally provide a measure of the signals quality for estimation purpose. We note here that, although all the results in this paper are relative to those two models, the method can be extended to higher order model under appropriate assumptions and additional measurements. However, additional measurements of state variables will be required as the system order increases.

III. Proposed Method

In the following we consider a general n-th order linear grid model, the relationship between the current I_{pcc} and the voltages V_{pcc} is given in the frequency domain as follows

$$I_{pcc}(j\omega) = G_{pcc}(j\omega)V_{pcc}(j\omega) + G_g(j\omega)V_g(j\omega), \quad (1)$$

where $G_{pcc}(j\omega)$ and $G_g(j\omega)$ are two transfer functions representing the impedance in the network.

The objective is to estimate the impedance transfer function between the PCC voltage and current $G_{pcc}(j\omega)$.

We assume that the grid voltage V_g is a pure harmonic wave with frequency content at 50 Hz and that the voltage and currents at the PCC have a sufficiently rich frequency content due to the inverter switching. Let $\hat{I}$ and $\hat{V}$ denote, respectively, the Discrete-Fourier Transforms (DFT) of the current and voltage signals at the PCC after removing the fundamental 50Hz component. Under these assumptions, an estimate of the transfer function can be obtained using Eq. (1) by taking the ratio of the current and voltage spectral signals as follows:

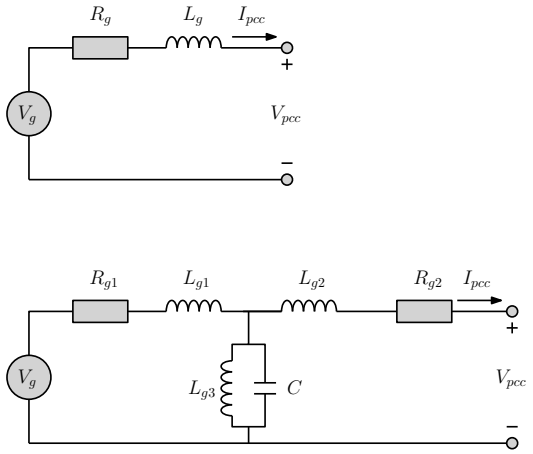

Fig. 2. Equivalent circuit for grid impedance. RL model (top) and LCL model (bottom).

$$G_{pcc}(j\omega) \approx \frac{\hat{I}_{pcc}(j\omega)}{\hat{V}_{pcc}(j\omega)}, \quad (2)$$

where $\hat{I}$ and $\hat{V}$ are the DFTs of the signals sampled at frequency f_s, the system frequency content ω is well below the Nyquist frequency ($2\pi f_s/2$). For brevity, the term "pcc" is omitted in the sequel.

A. Network Structure Identification

The first objective in the identification process is to determine the order of the system and therefore the structure of the grid, based on the measured data set. We employ a two step approach based on singular value decomposition (SVD) of the system Hankel matrix.

The first step consists on constructing the Hankel matrix using the estimated frequency response as per equation 2.

$$H = \begin{bmatrix} h_1 & h_2 & \dots & h_r \\ h_2 & h_3 & & h_{r+1} \\ \vdots & & \ddots & \vdots \\ h_r & h_{r+1} & \dots & h_{2r-1} \end{bmatrix},$$

where index r is chosen to be greater than the system order and the elements h_k are values of the system impulse response at different times and are calculated as,

$$h_k = \frac{1}{N}\sum_{n=0}^{N-1} G(e^{j\omega_n})e^{j2\pi kn/N}, \quad (3)$$

where N is the number of frequency samples. The resulting matrix captures the dynamics of the underlying system.

Next the singular values of the Hankel matrix is used to identify the number of dominant poles and hence the order of the transfer function. The singular value decomposition (SVD) approach provides insights into the relationship between input and output signals in system identification. Specifically, the singular values capture the magnitude and

complexity of the system's dynamics, aiding in the identification of dominant poles and separating them from the noise. The left singular vectors reveal the input-output relationship assisting in input excitation design. The right singular vectors offer insight into output sensitivity, model structure identification, and model order estimation. By analysing these matrices, valuable information about the system's behaviour, input-output relationships, and model characteristics can be extracted, enabling the system identification process.

To estimate the transfer function order accurately, the singular values obtained from SVD are sorted in descending order. A dramatic decrease in the singular values can be associated with the noise formed by small singular values, thus determining the order of the transfer function and therefore the grid structure.

B. Estimating the transfer function coefficients

Once we have determined the order of the transfer function, we can proceed to estimate the parameters. Here we consider the case of LCL grid, depicted in figure 2, however the estimation method can be readily applied to other configurations as well. From the Kirchhoff laws we can derive a relationship between the converter current, I, and the voltages V, which in Laplace domain is expressed as follows:

$$\begin{aligned} I(s) &= \frac{A(s^3)}{B(s^4)}V(s) + \frac{ks}{B(s^4)}V_g(s) \\ &= G(s)V(s) + G_g(s)V_g(s), \end{aligned} \tag{4}$$

where $A(s^3)$ and $B(s^4)$ denote polynomial of order 3 and 4, respectively, and k is a coefficient that makes $B(s)$ a monic polynomial, i.e. with the highest degree coefficient as 1.

In order to estimate the transfer function $G(s)$ we assume that the unknown grid voltage V_g is composed by a unique harmonic wave at 50Hz, and with negligible other frequency content. Additionally we assume the transfer function to be stable and neglect the transient response from the data set.

The transfer function $G(j\omega)$ can then be decomposed into real and imaginary parts as follows,

$$G(j\omega) = \frac{A((j\omega)^3)}{B((j\omega)^4)} \approx \frac{\hat{I}_{pcc}(j\omega)}{\hat{V}_{pcc}(j\omega)} = r_r(\omega) + jr_i(\omega), \tag{5}$$

or,

$$A((j\omega)^3) = (r_r(\omega) + jr_i(\omega))B((j\omega)^4), \tag{6}$$

where A and B are the nominator and denominator polynomials respectively, and r_r and r_i are, the real and imaginary parts of the I-over-V ratio at each frequency. Next we rewrite explicitly the terms of A and B:

$$\begin{aligned} A((j\omega)^3) &= a_3(j\omega)^3 + a_2(j\omega)^2 + a_1(j\omega) + a_0 \\ &= (r_r(\omega) + jr_i(\omega))((j\omega)^4 + b_3(j\omega)^3 + b_2(j\omega)^2 \\ &\quad + b_1(j\omega) + b_0). \end{aligned}$$

we then define parameter vector, x, which captures the polynomial coefficients of A and B as

$$x := \begin{bmatrix} b_3 & b_2 & b_1 & b_0 & a_3 & a_2 & a_1 & a_0 \end{bmatrix}^T.$$

Subsequently, Eq. 6 transforms into the following form:

$$\underbrace{\omega^4 \begin{bmatrix} r_r \\ r_i \end{bmatrix}}_{z(\omega)} = \underbrace{\begin{bmatrix} -r_i\omega^3 & r_r\omega^2 & r_i\omega & -r_r & 0 & -\omega^2 & 0 & 1 \\ r_r\omega^3 & r_i\omega^2 & -r_r\omega & -r_i & -\omega^3 & 0 & \omega & 0 \end{bmatrix}}_{H(\omega)} x, \tag{7}$$

where frequency dependency of r_i and r_r are omitted for brevity.

Eq. 7 is an algebraic equality of the form $z(\omega) = H(\omega)x$, where z and H both depend on the frequency, whereas x is a constant parameter vector.

This prompts to employ the recursive least squares method (RLS) on frequency domain data to estimate the parameter vector and consequently the entire transfer function $G(s)$. The RLS algorithm operates from the lowest frequency (DC) up to a specific frequency ω_{max} ($\omega_{max} < 2\pi f_s/2$), continually updating the parameter estimation vector $\hat{x}$ through the following iterative update law:

$$\hat{x}_{n+1} = \hat{x}_n + K(z(\omega_n) - H(\omega_n)\hat{x}_n), \tag{8}$$

where subscript n captures the index of frequency points used for the estimation, and the matrix K is the optimal gain matrix derived by the following equation

$$K = PH^T(HPH^T + R)^{-1}, \tag{9}$$

where R is the covariance matrix on the $z(\omega)$, and P is the covariance matrix of the estimate given by,

$$P = (I - KH)P(I - KH)^T + KRK^T. \tag{10}$$

C. Data quality analysis

In identifying system structure and parameters we assumed that the system was sufficiently persistent excited by the input, that is the collected input and output data were sufficiently rich in term of frequency content for the identification to be effective. This is however not always guaranteed and the data richness has to be assessed before employing the data for the identification process.

Informativeness of a frequency component refers to how much value it adds to the estimation of the parameters [27]. As previously defined, the relationship between vector $z(\omega)$, and the parameter vector x, is given by the following linear equation,

$$z(\omega) = H(\omega)x, \quad z \in \mathbb{R}^2,\ H \in \mathbb{R}^{2\times m},\ x \in \mathbb{R}^m. \tag{11}$$

Any vector x lying in the null-space of H has no effect on the measurements. In other words, if x^* is the least-squares solution to Eq. 11, adding any vector to x^* that belongs to the null-space of H, is still a valid solution. More rigorously,

$$H(x^* + x_{nH}) = Hx^*, \tag{12}$$

where $x_{nH} \in \text{null}(H)$ and $x = H^\dagger z$. The dependency on ω is omitted for clarity.

To have a numerically robust and precise estimation of the parameter vector x over a set of frequency points, the null-spaces of H's at different frequencies, i.e. null$(H(\omega_n))$, must cross one another. Since H is a 2-by-m matrix, where m is the dimension of parameters, the null-space of H has order of m-2. That is, the null-space is a hyperline in the parameter space. Fig. 3 graphically illustrates this concept. The point x_i^*'s denote the least square solutions to $z(\omega_n) = H(\omega_n)x_n$, and lines represent the null-spaces of each frequency.

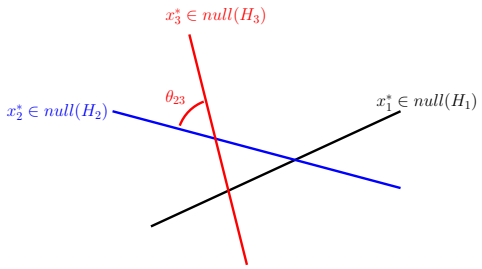

Fig. 3. Graphical representation of the null-space crossings.

For a given frequency ω_n, the minimum relative-crossing-angle in which the null-space of $H(\omega_n)$ crosses all other null-spaces can be calculated as

$$\theta_{ij}(\omega_n) = \min_{\omega_j} \angle(\text{null}(H_i),\ \text{null}(H_j)), \tag{13}$$

where $\angle$ denotes the principal angle between two subspaces (see Theorem 1 in [28]). The larger the angle is (up to 90°), the more information is introduced by the new direction of null$(H(\omega_n))$ [2].

Fig. 4 shows the calculation result of informativeness of frequency components for the LCL-type grid impedance estimation. The red curve illustrates the subspace angle of each frequency with respect to all other frequencies, which can be interpreted as information richness of each frequency. As illustrated in the plot, lower frequency and resonance neighborhood components provide the main contribution to the parameter estimation.

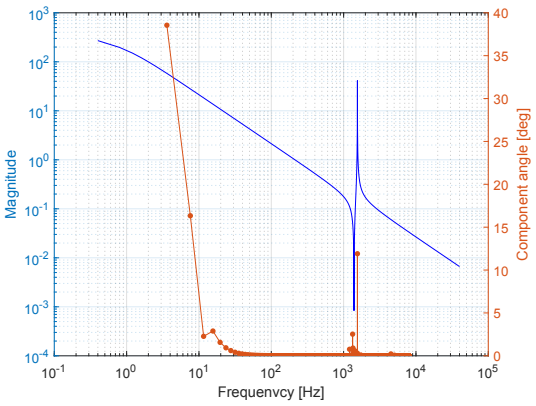

Fig. 4. Evaluation of the frequency content richness for the LCL grid type: (blue) the magnitude of the impedance transfer function, (red) relative degree (informativeness) of the frequency content.

D. Algorithm steps

The method workflow, depicted in Fig. 5, is composed by three main blocks consisting of: signal acquisition and processing, data analysis and structure and parameter identification. In the first block the PCC currents and the voltages signal are measured. The measurements are then pre-processed to remove noise and the 50Hz component. Then the Discrete Fourier Transform (DFT) is computed. The resulting frequency domain data are then fed into the network identification unit, where the Hankel matrix is constructed and decomposed using singular value decomposition in order to identify the impedance type, i.e. RL, LCL, and etc. Once the type is known, a linear model relating the unknown parameters to the measurements, i.e. $z(\omega) = H(\omega)x$, can be built. The generalized condition number of $H(\omega)$ matrix is a useful measure in assessing the reliability of the solution at the given frequency. If the condition number is large, the matrix is close to being singular, and thus, the corresponding frequency component is discarded. In addition, an analysis of data informativeness is performed on the data to evaluate the contribution of each frequency component to the grid parameter estimation. The frequency components that add no or limited information are discarded. If the number of informative frequencies is less than a threshold, the problem is considered infeasible, meaning that the frequency content is not rich enough to perform the grid impedance estimation; otherwise, the impedance estimation process is then carried out over the informative frequency set.

In case of constant impedance the data evaluation and identification process can be carried out offline. For variable grid impedance all described modules can be run efficiently online.

IV. Simulation Results

The effectiveness and accuracy of the proposed solutions is evaluated using field data from MV drives including voltage-source and current source converters for both balanced and unbalanced grid scenarios.

We consider a frequency range from DC to $f_{max} = 4kHz$ below the Nyquist frequency (see Fig. 6). The estimation result of the impedance transfer function is illustrated in Fig. 6. As we can see, the estimated transfer function fits in most of the frequency range, especially near the resonance region. Fig. 7 depicts the estimation results of the 8 polynomial coefficients as the frequency sweeps from DC to ω_{max}. It can be observed that the estimation slow down its learning process as soon as the resonance frequency 1500Hz is surpassed.

Fig. 8 shows the final converged values of the polynomial coefficients with their corresponding converged 6 standard deviations (6σ) bound.

A. RL-type grid

As a demonstrative example, we consider an RL type grid, resulting in the impedance transfer function being a first order system with two unknown parameters: R and L. Fig. 9 illustrates the estimation result of R and L parameters as

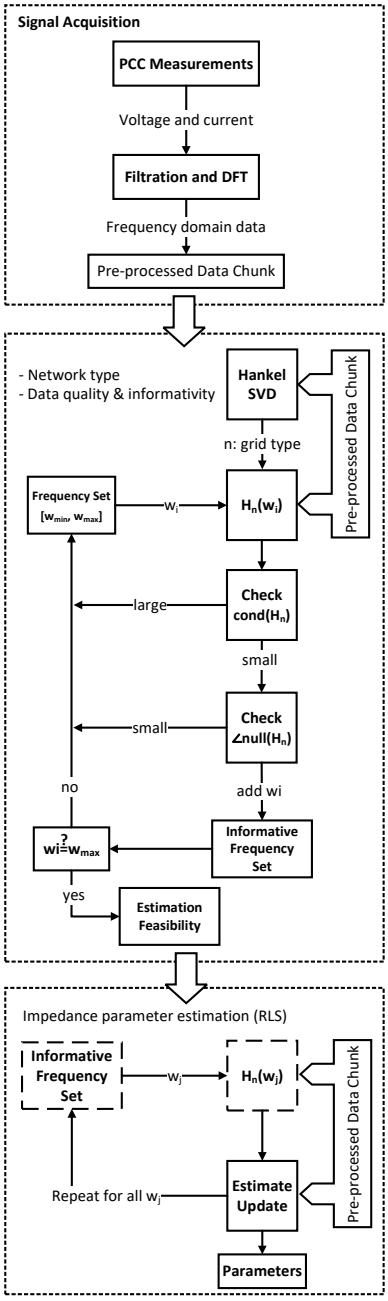

Fig. 5. Estimation method steps.

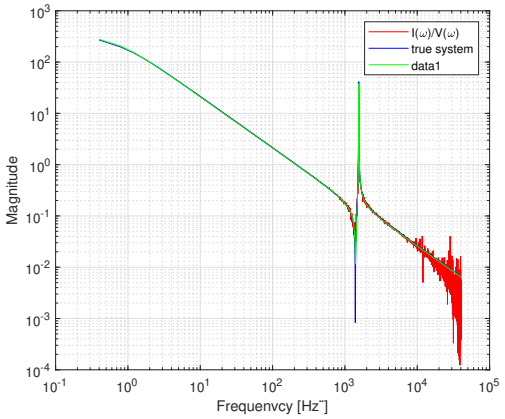

Fig. 6. Simulation result of the transfer function estimation using RLS method.

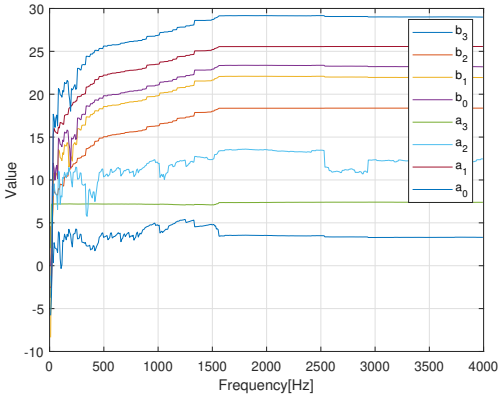

Fig. 7. Estimation of the polynomial coefficients (in logarithmic scale for better visibility) as the frequency proceeds.

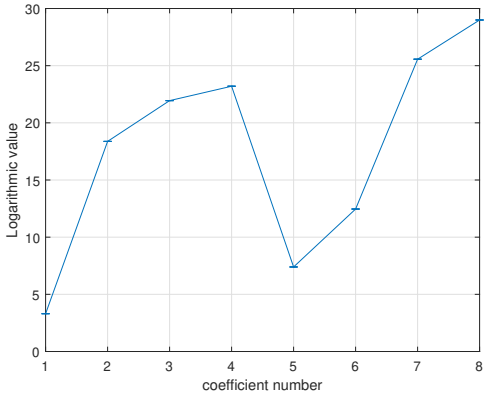

Fig. 8. The final coefficient values and their corresponding 6σ bound on logarithmic scale.

the frequency sweeps from zero to ω_{max}. Here, the maximum frequency is set to $\frac{2}{3}\omega_{\text{Nyquist}}$ with the sampling time $T_s = 1$ms and $N = 1000$ samples in the DFT. The covariance matrix P is used to give an estimate of the confidence interval on the estimated parameters. The six-sigma interval, i.e. $\pm 3\sigma$, is plotted in dashed lines in Fig. 9. The 3σ bound on R and L is approximately 2% and 0.1%, respectively.

V. Conclusion

This paper proposes a comprehensive, frequency domain based method to identify the structure and parameters of an unknown electric grid, based on voltage and current measurements. The method is based on a recursive least square (RLS)

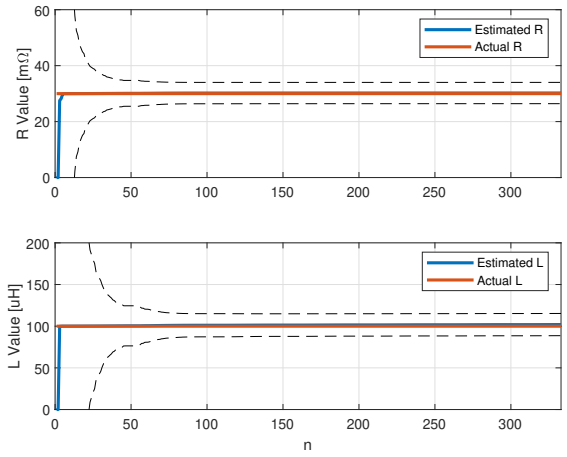

Fig. 9. Recursive estimation of the grid impedance (R and L) versus different number of frequency samples $\omega_n = n\frac{2\pi}{NT_s}$. The dashed curves denote the $\pm 3\sigma$ bound.

formulation in frequency domain resulting in an accurate and computationally efficient solution. Additionally, a data analysis is provided to classify the input output data and asses their quality and effectiveness for the identification process. The method has been successfully tested on field data, and it has demonstrated its potential to support diagnostic and control design for power conversion applications. In future work, for the case of limited data informativeness, we plan to define a region in the parameter space whose size will be determined by the data frequency content. This will provide a direct correlation between the data quality and the identification accuracy, and hence define a fingerprint of the data that can guarantee a reliable identification.

REFERENCES

[1] C. Li, M. Molinas, O. B. Fosso, N. Qin, and L. Zhu, "A data-driven approach to grid impedance identification for impedance-based stability analysis under different frequency ranges," in *2019 IEEE Milan PowerTech*, 2019, pp. 1–6.

[2] B. Hoseinzadeh, C. L. Bak, and F. Blaabjerg, "Impact of grid impedance variations on harmonic emission of grid-connected inverters," in *2017 IEEE Manchester PowerTech*, 2017, pp. 1–5.

[3] J. De Kooning, J. Van de Vyver, J. D. De Kooning, T. L. Vandoorn, and L. Vandevelde, "Grid voltage control with distributed generation using online grid impedance estimation," *Sustainable Energy, Grids and Networks*, vol. 5, pp. 70–77, 2016.

[4] N. Mohammed, M. H. Ravanji, W. Zhou, and B. Bahrani, "Online grid impedance estimation-based adaptive control of virtual synchronous generators considering strong and weak grid conditions," *IEEE Transactions on Sustainable Energy*, vol. 14, no. 1, pp. 673–687, 2023.

[5] M. Cespedes and J. Sun, "Adaptive control of grid-connected inverters based on online grid impedance measurements," *IEEE Transactions on Sustainable Energy*, vol. 5, no. 2, pp. 516–523, 2014.

[6] A. Ghanem, M. Rashed, M. Sumner, M. A. El-sayes, and I. I. I. Mansy, "Grid impedance estimation for islanding detection and adaptive control of converters," in *8th IET International Conference on Power Electronics, Machines and Drives (PEMD 2016)*, 2016, pp. 1–6.

[7] W. I. BOWER and M. ROPP, "Evaluation of islanding detection methods for utility-interactive inverters in photovoltaic systems." [Online]. Available: https://www.osti.gov/biblio/806700

[8] S. Liu, Y. Li, and J. Xiang, "An islanding detection method based on system identification," in *The 27th Chinese Control and Decision Conference (2015 CCDC)*, 2015, pp. 5515–5520.

[9] N. Mohammed, M. Ciobotaru, and G. Town, "Fundamental grid impedance estimation using grid-connected inverters: a comparison of two frequency-based estimation techniques," *IET Power Electronics*, vol. 13, no. 13, pp. 2730–2741, 2020.

[10] J. Kukkola, M. Routimo, and M. Hinkkanen, "Real-time grid impedance estimation using a converter," in *2019 IEEE Energy Conversion Congress and Exposition (ECCE)*, 2019, pp. 6005–6012.

[11] N. Hoffmann and F. W. Fuchs, "Minimal invasive equivalent grid impedance estimation in inductive–resistive power networks using extended kalman filter," *IEEE Transactions on Power Electronics*, vol. 29, no. 2, pp. 631–641, 2014.

[12] J. Fang, H. Deng, and S. M. Goetz, "Grid impedance estimation through grid-forming power converters," *IEEE Transactions on Power Electronics*, vol. 36, no. 2, pp. 2094–2104, 2021.

[13] S. Mastellone, P. Al-Hokayem, and P. Raboni, "Islanding detection in an electrical power grid," Patent 10 852 336, October, 2018.

[14] M. Ciobotaru, R. Teodorescu, P. Rodriguez, A. Timbus, and F. Blaabjerg, "Online grid impedance estimation for single-phase grid-connected systems using pq variations," in *2007 IEEE Power Electronics Specialists Conference*, 2007, pp. 2306–2312.

[15] N. Mohammed, M. Ciobotaru, and G. Town, "An improved grid impedance estimation technique under unbalanced voltage conditions," in *2019 IEEE PES Innovative Smart Grid Technologies Europe (ISGT-Europe)*, 2019, pp. 1–5.

[16] X. Sun, J. Chen, J. M. Guerrero, X. Li, and L. Wang, "Fundamental impedance identification method for grid-connected voltage source inverters," *IET Power Electronics*, vol. 7, no. 5, pp. 1099–1105, 2014.

[17] D. D. Reigosa, F. Briz, C. B. Charro, and J. M. Guerrero, "Islanding detection in three-phase and single-phase systems using pulsating high-frequency signal injection," *IEEE Transactions on Power Electronics*, vol. 30, no. 12, pp. 6672–6683, 2015.

[18] A. Vijayakumari, A. Devarajan, and N. Devarajan, "Decoupled control of grid connected inverter with dynamic online grid impedance measurements for micro grid applications," *International Journal of Electrical Power Energy Systems*, vol. 68, pp. 1–14, 2015.

[19] M. Ciobotaru, R. Teodorescu, and F. Blaabjerg, "On-line grid impedance estimation based on harmonic injection for grid-connected pv inverter," in *2007 IEEE International Symposium on Industrial Electronics*, 2007, pp. 2437–2442.

[20] L. Asiminoaei, R. Teodorescu, F. Blaabjerg, and U. Borup, "Implementation and test of an online embedded grid impedance estimation technique for pv inverters," *IEEE Transactions on Industrial Electronics*, vol. 52, no. 4, pp. 1136–1144, 2005.

[21] ——, "A digital controlled pv-inverter with grid impedance estimation for ens detection," *IEEE Transactions on Power Electronics*, vol. 20, no. 6, pp. 1480–1490, 2005.

[22] S. A. S. Hesari, M. Hamzeh, and H. Toobak, "Performance assessment of an impedance based islanding detection method in a distribution network with multiple pv inverters," in *2011 International Conference on Power and Energy Systems*, 2011, pp. 1–6.

[23] G. Shen, J. Zhang, X. Li, C. Du, and D. Xu, "Current control optimization for grid-tied inverters with grid impedance estimation," in *2010 Twenty-Fifth Annual IEEE Applied Power Electronics Conference and Exposition (APEC)*, 2010, pp. 861–866.

[24] R. Luhtala, T. Roinila, and T. Messo, "Implementation of real-time impedance-based stability assessment of grid-connected systems using mimo-identification techniques," *IEEE Transactions on Industry Applications*, vol. 54, no. 5, pp. 5054–5063, 2018.

[25] M. Sumner, B. Palethorpe, D. Thomas, P. Zanchetta, and M. Di Piazza, "A technique for power supply harmonic impedance estimation using a controlled voltage disturbance," *IEEE Transactions on Power Electronics*, vol. 17, no. 2, pp. 207–215, 2002.

[26] M. Céspedes and J. Sun, "Online grid impedance identification for adaptive control of grid-connected inverters," in *2012 IEEE Energy Conversion Congress and Exposition (ECCE)*, 2012, pp. 914–921.

[27] A. Rezaeizadeh, "Set membership identification and control of an iterative process," in *2019 18th European Control Conference (ECC)*, 2019, pp. 36–41.

[28] Åke Björck and G. H. Golub, "Numerical methods for computing angles between linear subspaces," *Mathematics of Computation*, vol. 27, no. 123, pp. 579–594, 1973.